EUROfusion

WPEDU-PR(18) 20508

AD Durif et al.

Impact of tungsten recrystallization on ITER-Like components for lifetime estimation

Preprint of Paper to be submitted for publication in
Journal of Nuclear Materials

This work has been carried out within the framework of the EUROfusion Consortium and has received funding from the Euratom research and training programme 2014-2018 under grant agreement No 633053. The views and opinions expressed herein do not necessarily reflect those of the European Commission.

Impact of tungsten recrystallization on ITER-Like components for lifetime estimation

A. DURIF[a,**], M. RICHOU[a,*], G.KERMOUCHE[b], M.LENCI[b], J-M. BERGHEAU[c]

[a] *CEA, IRFM, F-13108 Saint-Paul-Lez-Durance, France*
[b] *École nationale supérieure des mines de Saint-Étienne, LGF, CNRS UMR 5307, 42023 Saint-Etienne cedex 2, France*
[c] *University of Lyon, Ecole Nationale d'ingénieurs de Saint-Etienne, LTDS, CNRS UMR 5513, 42023 Saint-Etienne, France*

Abstract

For ITER divertor, plasma facing components are made with tungsten as armor material. In previous papers, it has been shown that plasma facing components are prone to crack, appearing in tungsten block during thermal cyclic heat loading. In order to predict component lifetime, a numerical simulation is proposed in this paper. With regard to previous studies, tungsten (raw and recrystallized) real mechanical behaviors are taken into account. To be used as inputs for numerical simulations, compression tests at different temperatures and strain rates were realized on raw and recrystallized tungsten. Raw tungsten tests reveal a linear elastic and ideal plastic behavior that is sensitive to strain rate. Concerning recrystallized tungsten, an elastic-viscoplastic behavior is observed on the entire explored temperature range (Up to 1150°C), that can be described by an elastic-plastic model with kinematic hardening. Manson-Coffin relationships are used to estimate the lifetime. When taking account real mechanical behaviors for raw tungsten and recrystallized tungsten, we show that lifetime estimation is mainly driven by recrystallized thickness in the component, by strain rate and finally by the ductile to brittle transition temperature.

Keywords: tungsten, damage, lifetime, compression test, mechanical behavior, plastic strain, recrystallization

1. Introduction

The fusion reaction could become a viable way to generate electricity. To perform this reaction, reactors confine magnetically plasma in a vacuum chamber. However, plasma confinement is imperfect and due to the magnetic plasma

*Corresponding author
**Principal corresponding author
Email addresses: alan.durif@cea.fr (A. DURIF), marianne.richou@cea.fr (M. RICHOU)

configuration, energy losses are directed toward the main wall, mainly on the lower part of the vessel called divertor. For the ITER (International Tokamak Experiment Reactor) divertor, plasma facing components have to withstand cyclic high heat flux (stationary and transient) up to 20 MW/m^2[1]. High Heat Flux (HHF) experimental campaigns were performed [2] and proved that actively cooled plasma facing components made with tungsten as armor material, bonded on a coper alloy tube as heat sink structural material are able to satisfy the ITER heat exhaust requirements (20 MW/m^2) [3]. However, due to high heat flux, strong temperature gradients are generated on a thickness of 7 mm, leading to extreme temperature values from 2000°C at the loaded surface to 700°C near the cooling tube [4]. 2000°C is large enough to alter the tungsten microstructure causing recrystallization and mechanical properties losses and then damages such as macro cracks in the material [2, 5, 6, 7]. It is thus necessary to identify which phenomena have to be taken into account to predict the lifetime of tungsten armored component, this identification is the aim of this paper. M.Li et al, pointed out that recrystallization is a key phenomenon regarding lifetime prediction [8, 9]. Indeed, they show that the loss of mechanical properties induced by recrystallization leads to an increase of plastic strain increment per thermal cycle. From Manson-Coffin relationship they conclude on the drastic reduction of the component lifetime. However, thermomechanical model uses by assumption an linear elastic and ideal plastic behavior for recrystallized tungsten. In this paper, it is proposed to investigate the effect of the actual mechanical behaviour of tungsten grades (in recrystallized and no recrystallized states) on lifetime prediction. For this, the model proposed by M. Li et al [8] is used and assumed mechanical behaviours of tungsten are replaced by the actual ones. In the first part of this paper, compressive tests of raw and recrystallized tungsten for different temperatures and strain rates are presented. The thermomechanical model is then described. Numerical simulations are performed to estimate the plastic strain increments depending on various parameters: thickness of the recrystallized layer and constitutive relations. Manson-Coffin relations are finally used to estimate the number of cycles to failure. A conclusion is finally brought on the key parameters that govern the lifetime prediction of plasma facing components.

2. High temperature compression tests

2.1. Materials and methods

ITER requirements request tungsten manufacturers to supply material with strong grains orientation [3]. Usually, oriented microstructure is obtained by a forming or rolling process. Rolling process involves grain orientation, strain rate sensitivity and promotes tungsten recrystallization. Microstructure change, such as recrystallization decreases significantly the mechanical properties of the material [10]. Compression tests are thus performed on rolling tungsten provided by Advance Technology and Materials (AT&M) which is one of the ITER tungsten grade suppliers. Tungsten samples are cylindrical (9*6mm^2) cut into

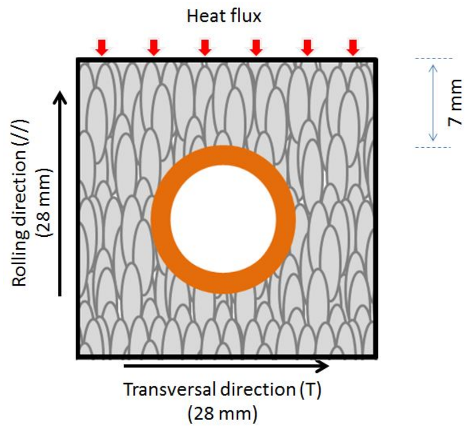

Figure 1: Theoretical grain microstructure on rolling tungsten block

tungsten blocks (28*28*12 mm^3). 24 samples were prepared. Samples are cut in the transversal direction (T) (Figure 1) and half of them are then annealed (15 hours at 1350°C) to obtain a recrystallized microstructure. Compression tests are performed on raw and recrystallized tungsten at 500°C, 750°C, 900°C and 1150°C. Experiments were achieved in argon atmosphere to avoid oxidation on surfaces samples. For each test, sample was coated with graphite and boron in order to avoid friction during the compression. Once samples reached test temperatures, they were maintained 10 minutes to ensure a homogeneous temperature in the whole sample. Two thermocouples were used for temperature measurements.

Compressive tests were performed for several strain rates for the same temperature range. Strain rates were chosen based on the expected thermal strain rate ($\dot{\varepsilon}^{th}$) in ITER (equation 1):

$$\dot{\varepsilon}^{th} = \frac{(T_s - T_0) * \alpha(T_s)}{\Delta t} \tag{1}$$

Where T_s corresponds to the block surface temperature and α corresponds to the thermal expansion coefficient (5.08.10-6 K^{-1} at 1400°C [10]). Previous simulations [4] show that at 20MW/m^2, the surface temperature can reach up to 1400°C in approximately 1.2s (t=1.2s). T_0 is representative of the initial temperature of the tungsten block under cooling condition before plasma shock (T_0=120°C) [8]. Finally, strain rate is estimated around 6.10^{-3} s^{-1}. Also, fast transient heat loadings are expected in ITER [11]. These particulars heat loadings (edges localized modes) have strong impact on the tungsten surface temperature. In this context it was decided to test samples also at higher strain rates (6.10^{-2}/s and 6.10^{-1}/s).

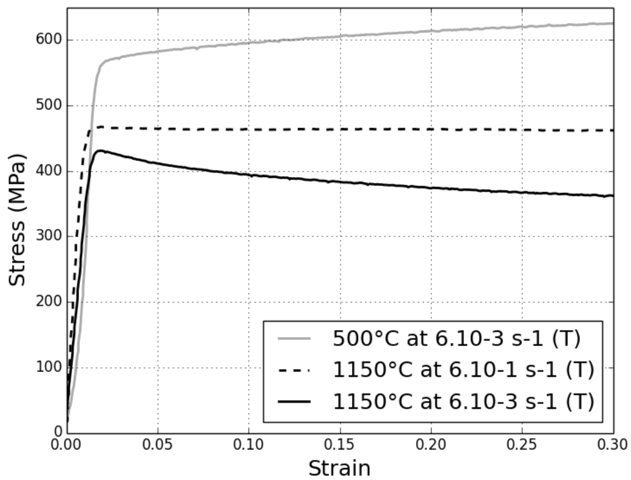

Figure 2: Stress-strain curves obtained on raw tungsten at 500°C at 6.10-3s-1 and 1150°C obtained at 6.10-3 s-1 and 6.10-1 s-1

2.2. Results

In Figure 2, stress-strain curves are plotted for 500°C (at 6.10^{-3} s^{-1}) and 1150°C (at 6.10^{-3} s^{-1} and 6.10^{-1} s^{-1}). Curves reveal that tungsten is ductile between 500°C and 1150°C and that tungsten has a linear elastic and ideal plastic behaviour. Moreover, yield stresses (estimated at 0.2%) decrease from 559 MPa at 500°C to 426 MPa at 1150°C, showing that temperature has an impact on tungsten mechanical property. Also, strain rate effect is observable, indeed, yield stresses (estimated at 0.2%) decrease from 459 MPa at $6.10^{-1}s^{-1}$ to 426 MPa at $6.10^{-3}s^{-1}$. To conclude, Figure 2 highlights that raw tungsten recrystallizes dynamically at 1150°C (at 6.10^{-3} s^{-1}). In this case, once the tungsten reached the yield stress, a stress decrease is noticed during the test.

In figure 3, stress-strain curves are plotted for 500°C at 6.10^{-3} s^{-1} and 1150°C (at 6.10^{-3} s^{-1} and at 6.10^{-1} s^{-1}). Recrystallized tungsten is ductile between 500°C and 1150°C. This clearly involves that Ductile to Brittle Transition Temperature (DBTT) is below 500°C. In the literature, several tungsten grades were studied and large differences were obtained concerning the estimation of the DBTT [12, 13]. In a further study this effect will be studied. The increase of temperature has a strong impact on mechanical properties of recrystallized tungsten. Yield stress (estimated at 0.2%) decreases from 61 MPa at 500°C to 49 MPa at 1150°C. Contrary to the linear elastic and ideal plastic case, described for raw tungsten, recrystallized tungsten exhibit a strong hardening. Once the yield stress is attained; stress has to be endlessly increased to ensure plastic strain. Tangent moduli obtained are presented in Table 2. Recrystallized tungsten is also sensitive to strain rate. Same quantitative results are obtained for each studied temperature. These observations lead to conclude that recrystallized

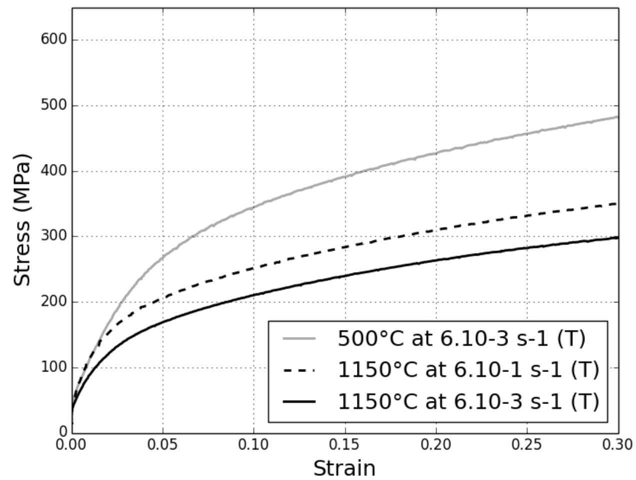

Figure 3: Stress-strain curves obtained on recrystallized tungsten at 500°C (at $6.10^{-3}s^{-1}$) and 1150°C (at $6.10^{-3}s^{-1}$ and at $6.10^{-1}s^{-1}$)

Table 1: Raw tungsten mechanical properties obtained under compressive and tensile tests

	Tensile test [14] (800°C, 10^{-4} s^{-1})	Compressive test (750°C, 6.10^{-3} s^{-1})
Yield stress (MPa)	579	552
Stress at 0.2 (MPa)	579	553

tungsten has elastic-viscoplastic behaviour.

Here below, correlation of obtained mechanical characteristics with other published characteristics [14] is presented. In Table 1, yield stresses and stresses values obtained at 0.2 at 750°C (representative of the described compressive test obtained at 6.10^{-3} s^{-1} on raw tunsgten) and at 800°C [14] (obtained on AT&M tungsten grade during tensile test at 10^{-4} s^{-1}) are presented. Comparable yield stresses (=5%) are obtained, revealing that plastic constitutive relation obtained in compression are representative to that obtained in traction.

3. Finite element analysis

3.1. Geometry, meshing

Geometry presented in Figure 4, is representative of an ITER divertor block. Thanks to the use of two symmetry planes only quarter part block is modelled. Dimensions are identical to the ones implemented in the numerical model used by M.Li et al [8] (28*14*6 mm^3). ANSYS 17.2 commercial finite element analysis code is used to perform this geometry. 8440 quadratic elements are used to mesh the 3D geometry.

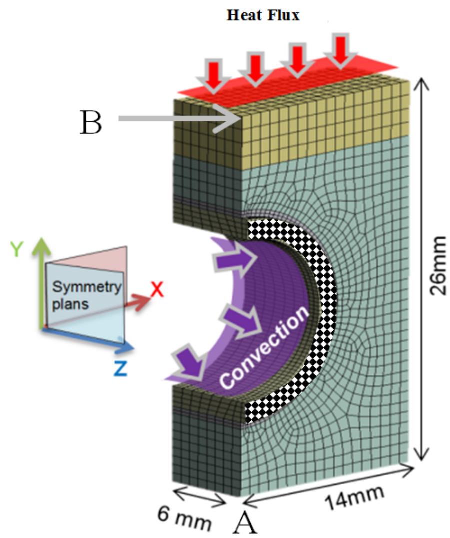

Figure 4: Numerical model

3.2. Materials properties

Based on described mechanical tests, tungsten is assumed to be linear elastic and ideal plastic. No hardening is modelled for this material. Despite the slight anisotropy effect [14], tungsten is assumed isotropic in this model. Elastic-visoplastic behaviour with hardening was observed for recrystallized tungsten. To take into account this in our upcoming simulations, kinematic hardening model are used. In stress space, kinematic hardening models allow a translation of the yield surface and hence that cyclic effects like softening, hardening or Bauschinger effect [15] can be modelled. Under mechanical cycling loadings, tungsten softening behaviour was highlighted in literature [16]. In this manner, use of kinematic hardening model is mandatory for recrystallized tungsten. Bilinear kinematic hardening model is used in simulations. This model assumes that the stress-strain curve can be described as two straight line segments. For the elastic part, slope is young modulus and for the plastic part, slope is tangent modulus. Tungsten mechanical properties obtained under compressive tests (yield stress and tangent modulus) used in dedicated simulations are summarized in Table2. Young modulus, heat conductivity and coefficient of thermal expansion used are those presented for the raw tungsten, recrystallized tungsten in [8]. Also, mechanical properties used for Cu-OFHC and CuCrZr are those presented in [8]. Stresses and strains generated in the both copper materials are not studied.

3.3. Studied cases

In this paper, several simulations are performed.

Table 2: Material properties

Material	Temperature (°C)	Strain rate (s^{-1})	Yield stress at 0.2% (MPa)	Tangent Modulus (MPa)
raw tungsten	500	6.10^{-3}	559	0
		6.10^{-1}	678	0
	1150	6.10^{-3}	426	0
		6.10^{-1}	459	0
recrystallized tungsten	500	6.10^{-3}	61	5913
		6.10^{-1}	46	9618
	1150	6.10^{-3}	49	3906
		6.10^{-1}	58	4985

1. The *Reference* simulation (**Ref**, Figure 5) assumes raw tungsten obtained experimentally at $6.10^{-3}s^{-1}$of strain rate.

2. Second simulation which aims to *analyse the effect of the strain rate* (**SR**, Figure 5); assumes raw tungsten and uses mechanical properties obtained experimentally at $6.10^{-1}s^{-1}$ of strain rate.

3. Another simulation which aims to *analyse the effect of tungsten recrystallization* (**RXX thickness 2**, Figure 5); assumes 2 mm thickness of recrystallized tungsten on the upper part of the model. 2 mm thickness of the recrystallized tungsten is chosen as it is representative to that observed on the center of the block after 300 high heat flux cycles [2]. This model uses, for raw tungsten and recrystallized tungsten, related mechanical properties obtained experimentally at 6.10^{-3} $s^{-1}$of strain rate.

4. Another simulation which aims to *analyse the effect of tungsten recrystallization thickness* (**RXX thickness 4**, Figure 5); assumes 4 mm thickness of recrystallized tungsten on the upper part of the model and uses, for raw tungsten and recrystallized tungsten, related mechanical properties obtained experimentally at $6.10^{-3}s^{-1}$ of strain rate. Conservative 4 mm thickness of the recrystallized tungsten is chosen as it is representative to that observed on the block edge after 300 high heat flux cycles [2].

5. Another simulation which aims to analyse the *effect of tungsten recrystallization combined to the effect of strain rate* (**SR+RXX**,) Figure 5); assumes 4 mm thickness of recrystallized tungsten on the upper part of the model and uses for raw tungsten and recrystallized tungsten related mechanical properties obtained experimentally at $6.10^{-1}s^{-1}$of strain rate.

3.4. Boundary conditions and thermal loads

As in M. Li et al model [8], one lower corner node (named A Figure 4) is constrained and free node displacements are allowed only in the pipe axial direction for pipe surface (surface with chequered pattern, Figure 4). For comparison, same thermal loads as M.Li et al are applied on the block upper surface. Convective boundary condition is applied to the cooling pipe inner surface. CEA routine [17], is used to calculate heat transfer coefficients taking into account

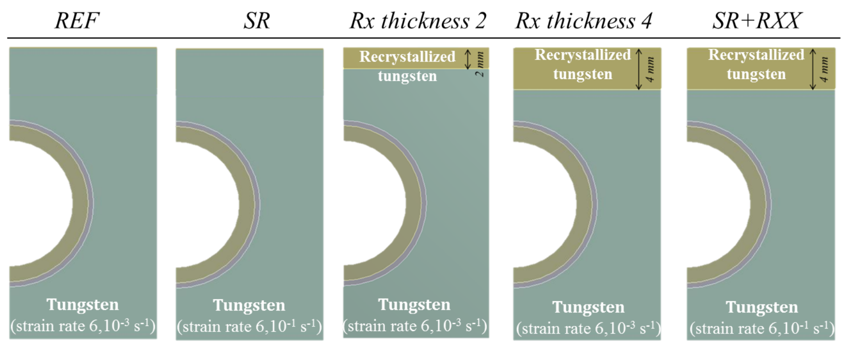

Figure 5: Simulations

Table 3: Representative heat transfer coefficient data used in simulations

T (°C)	50	100	150	200	250	290
Heat transfer coefficient ($kW/m^2.°C$)	98.6	108.2	115.0	120.0	124.2	207.1

coolant conditions (pressure 3.3 MPa, temperature 120°C and water velocity 12m/s). Calculated coefficients are presented in Table 3 and are representative of those given by M.Li et al.

4. Finite element results

4.1. Temperature field

Thermal loadings at 20 MW/m^2 involve strong temperature gradient on a thickness of 7 mm leading to extreme temperature values (2227°C) at the loaded surface to 700°C at the cooling tube (Figure 6).

4.2. Mechanical response

Maximum plastic strains are expected to be observed in the center of the block where the maximum temperature gradient is located (point B, Figure 4). Indeed, during experimental campaigns, this region corresponds to macro crack opening location [2]. Mechanical model used in simulations stabilized quickly. Indeed, Figure 7 highlights the evolution of the plastic strain at point B (Figure 4) for simulation **Ref**. After 4 thermal cycles, mechanical response becomes stable. Same quantitative observation is obtained for all performed simulations. Consequently, following mechanical results are the ones obtained at the 5^{th} cycle. Equivalent plastic strain increment ($\Delta\varepsilon_p$) is estimated for each simulation in order to perform life-time calculations. $\Delta\varepsilon_p$ corresponds to half of the plastic strain generated over the 5^{th} thermal cycle [8]. For the different simulations, $\Delta\varepsilon_p$ is summarized in Table 4. Figure 8 shows the evolution of plastic strain over thermal cycle for each simulation.

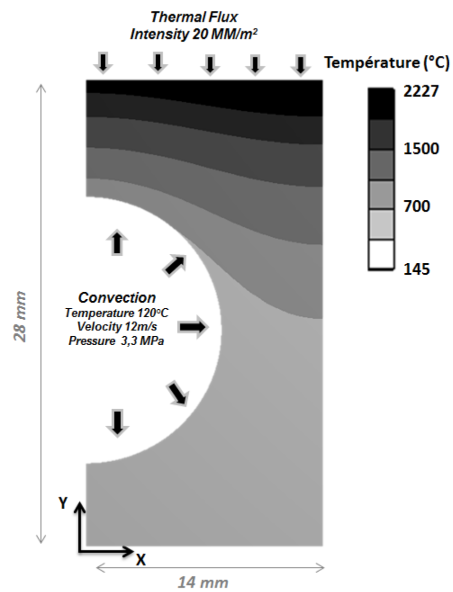

Figure 6: Tungsten temperature at 20MW/m^2

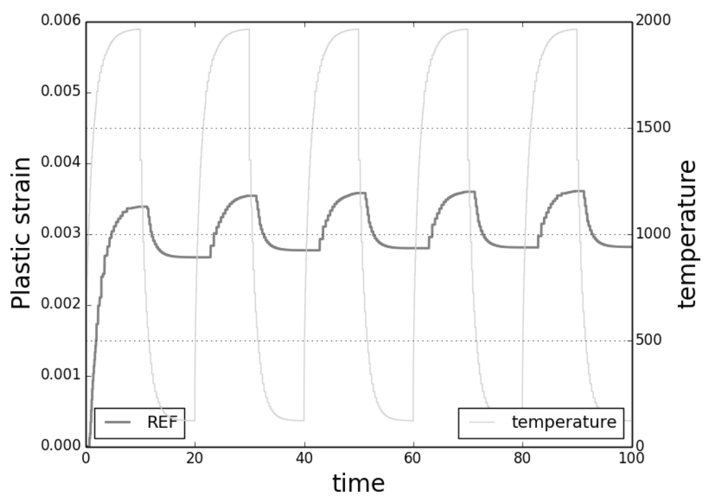

Figure 7: Plastic strain and temperature for **Ref** simulation at point B

Table 4: Equivalent plastic strain increments ($\Delta\varepsilon_p$) obtained for each simulation after 5th thermal cycle

	Ref	**SR**	**RXX thickness 2**	**RXX thickness 4**	**SR +RXX**
Strain rate (s^{-1})	6.10^{-3}	6.10^{-1}	6.10^{-3}	6.10^{-3}	6.10^{-1}
$\Delta\varepsilon_p$ (%)	0.08	0.03	0.65	0.53	0.62

Table 5: Numerical life time prediction assuming DBTT at 500°C

$\Delta\varepsilon p<500$: Part of $\Delta\varepsilon_p$which appeared bellow the DBTT (%) fixed at 500°C

$N1_{<500}$: number of cycles to failure obtained below the DBTT fixed at 500°C

$N2_{>500}$: number of cycles to failure obtained above the DBTT fixed at 500°C

N_{f500}: Final life time estimation assuming DBTT at 500°C

	Ref	**SR**	**RXX thickness 2**	**RXX thickness 4**	**SR +RXX**
$\Delta\varepsilon_{p<500}$ (%)	36	49	13	13	12
$N_{1<500}$	1311	15243	33	62	34
$N_{2>500}$	1431025	22100685	1926	4630	2226
N_{f500}	1310	15232	32	61	33

4.2.1. Raw tungsten

According to transient calculations, $\Delta\varepsilon_p$ is equal to 0.08% for simulation **Ref** and 0.03% for simulation **SR** (Table 4). These reveal that strain rate has an important effect on the mechanical plastic strain estimation for raw tungsten.

4.2.2. Recrystallized tungsten

Between **RXX thickness 4** and M. Li et al simulations, the only change is the mechanical tungsten behaviours inputs. Comparing $\Delta\varepsilon_p$ obtained for the **RXX thickness 4** simulation (0.65%), with the ones obtained by M. Li et al [8] (0.325%.), one can note that use of the actual elastic-plastic behaviour of recrystallized tungsten involves important $\Delta\varepsilon_p$ difference (nearly twice higher). As presented by M.Li et al [8], Figure 8 reveals that tungsten recrystallization thickness play an important role on the evolution of material plastic strain. Indeed, $\Delta\varepsilon_p$ obtained for **Ref** simulation is seven times higher than the one obtained for simulation **RXX thickness 2** and eight higher than the one obtained for simulation **RXX thickness 4**. According to Figure 8, $\Delta\varepsilon_p$ is equal to 0.65% for **RXX thickness 4** simulation and 0.63% for **SR+RXX** simulation (Table 4). These reveal that, strain rate has negligible effect on the mechanical plastic strain estimation for recrystallized tungsten.

5. Discussion on lifetime prediction

In order to optimize the use of plasma facing components in thermonuclear reactors and so ensure the mechanical vacuum chamber integrity over plasma

Table 6: Numerical life time prediction assuming DBTT at 350°C

$\Delta\varepsilon_{p<350}$: Part of $\Delta\varepsilon_p$ which appeared bellow the DBTT (%) fixed at 350°C

$N_{1<350}$: number of cycles to failure obtained below the DBTT fixed at 350°C

$N_{2>350}$: number of cycles to failure obtained above the DBTT fixed at 350°C

N_{f350}: Final life time estimation assuming DBTT at 350°C

	Ref	**SR**	**RXX thickness 2**	**RXX thickness 4**	**SR +RXX**
$\Delta\varepsilon_{p<350}$ (%)	22	46	7	6	5
$N_{1<350}$	6552	18421	269	497	267
$N_{2>350}$	934347	19714176	1441	3442	1658
N_{f350}	6211	18404	227	434	230

shocks, numerical life time prediction has to be performed. In the past, high heat flux experimental campaigns achieved and revealed that macro crack appears in tungsten block shortly after 300 thermal cycles (ITER requirements) [3]. In the literature, experiments are commonly performed to link equivalent plastic strain increments ($\Delta\varepsilon_p$) directly to number of cycles to failure (N_f) [18]. Manson-Coffin power law is used to estimate lifetime [19]. Low cycle fatigue data are available for several tungsten grades. Although, these are not corresponding to the studied tungsten grade, these experimental data are used in this paper in order to estimate life time.

Here, three Manson-Coffin relations displayed by M.Li et al [8] are used in this study. Two of them are given for raw tungsten (stress-relieved) at two different temperatures (23°C and 815°C) and the third one is given for recrystallized tungsten (annealed) at 815°C.

To study the effect of the DBTT on components life time, numbers of cycles to failure calculations are performed at two different DBTTs (350°C and 500°C) [12, 13]. In this manner, part of $\Delta\varepsilon_p$ generated above the DBTT are used to estimate number of cycles to failure (N_2) with the related Manson-Coffin relations obtained at 815°C (annealed for recrystallized and stress relieved for raw tungsten) and the part of $\Delta\varepsilon_p$ generated below the DBTT will be used to estimate number of cycles to failure (N_1) with the Manson-coffin relation obtained at 23°C. Then, thanks to the following relation (equation 2), related N_1 and N_2 are used to estimate final number of cycles to failure (N_f) [8]:

$$\frac{1}{Nf} = \frac{1}{N1} + \frac{1}{N2} \tag{2}$$

Depending on simulations, Figure 8 shows that during transient (heating and cooling) phases, part of $\Delta\varepsilon_p$ appears below DBTTs. No plastic strain occurs below DBTTs during the heating phase for **Ref** and **SR** simulations. This reveals that quantitatively, cooling phase has stronger impact on the monoblock damage process. Concerning the other simulations, Figure 8 reveals that heating and cooling phase play an equivalent role on the monoblock damage process.

Table 5 and Table 6 summarize related numbers of cycles to failure ob-

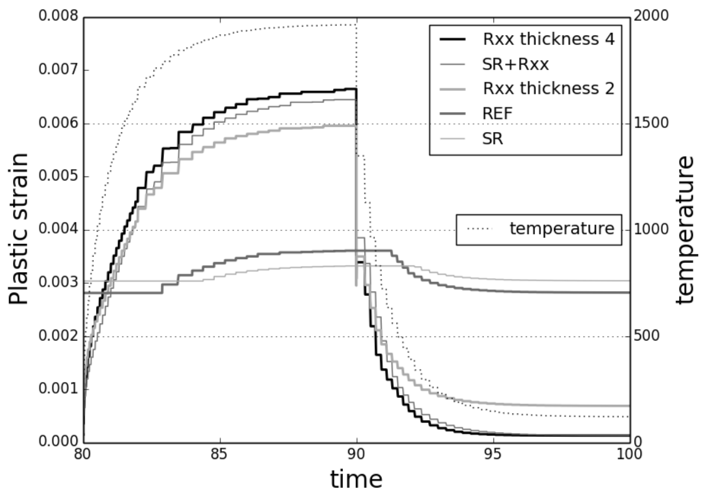

Figure 8: Evolution of point B temperature and of equivalent plastic strain occurring for each simulation at the 5th thermal cycle

tained for each simulation. Component lifetime is drastically reduced due to recrystallization. Also, tungsten thickness recrystallized layer play a role on the component life time. In this way, recrystallization phenomenon will be investigated further in the future to better define and model this phenomenon. Besides, Table 5 and Table 6 reveal an effect of DBTT on components life time. Indeed, for the simulation **RXX thickness 2**, component life time reduces significantly from 424 to 61 cycles. The actual DBTT of rolled tungsten should be consequently acuratly defined. In the case of **RXX thickness 2**, calculated number of cycles to failure is consistent to the one observed experimentally for the same recrystallized layer condition [2]. Also, presented calculations reveal significant effect of strain rate on the raw tungsten component life time; this is not the case for component with a recrystallized tungsten layer. In future, viscoplasticity of tungsten could be neglected for simulations with recrystallized tungsten.

6. Conclusion

This paper proposes to estimate tungsten armoured component life time taking into account actual mechanical behaviour of raw and recrystallized tungsten. For that, compressive tests were performed at several temperatures from 500°C to 1150°C and at several strain rates from 6.10^{-1} s^{-1} to 6.10^{-3} s^{-1}. Raw tungsten tests reveal an elastic-plastic behavior that is sensitive to strain rate. Concerning recrystallized tungsten, it showed an elastic-viscoplastic behavior on the entire explored temperature range. This behavior was described by an elastic-plastic model with kinematic hardening constitutive relation in the modeling.

Up to now, in the literature, mechanical behavior of tungsten and recrystallized tungsten were assumed as linear elastic and ideal-plastic using mechanical data displayed in [10]. Using mechanical behaviors experimentally obtained which are implemented in finite element modeling simulations; we show that higher numbers of cycles to failure are obtained. Simulations reveal that: recrystallization phenomenon, DBTT and strain rate have major effect on the component life time. Also, consistent life time estimations were obtained compared to that observed in literature. These observations highlight that in the future, more accurate estimations could be performed by using dedicated mechanical model capable of taking into account the actual behaviour of tungsten and modelling tungsten recrystallization phenomenon under thermal loadings.

7. Acknowledgements

The authors express their deep gratitude to Séverine Girard who performed compressive tests at Ecole Nationale Supérieure des Mines de Saint-Etienne. This work has received CEA funding from the "Programme Transverse de Compétence, Matériaux et Procédés (PTC-MP). This work has been carried out within the framework of the EUROfusion Consortium and has received funding from the Euratom research and training programme 2014-2018 under grant agreement No 633053. The views and opinions expressed herein do not necessarily reflect those of the European Commission.

---

[1] K. Ezato et al., "Progress of ITER full tungsten divertor technology qualification in Japan," Fusion Eng. Des., vol. 98–99, pp. 1281–1284, Oct. 2015.

[2] G. Pintsuk et al., "Characterization of ITER tungsten qualification mock-ups exposed to high cyclic thermal loads," Fusion Eng. Des., vol. 98–99, pp. 1384–1388, Oct. 2015.

[3] T. Hirai et al., "Status of technology R&D for the ITER tungsten divertor monoblock," J. Nucl. Mater., vol. 463, pp. 1248–1251, Aug. 2015.

[4] T. Hirai et al., "Use of tungsten material for the ITER divertor," Nucl. Mater. Energy.

[5] P. Gavila et al., "High heat flux testing of mock-ups for a full tungsten ITER divertor," Fusion Eng. Des., vol. 86, no. 9–11, pp. 1652–1655, Oct. 2011.

[6] B. Riccardi, R. Giniatulin, N. Klimov, V. Koidan, and A. Loarte, "Preliminary results of the experimental study of PFCs exposure to ELMs-like transient loads followed by high heat flux thermal fatigue," Fusion Eng. Des., vol. 86, no. 9–11, pp. 1665–1668, Oct. 2011.

[7] G. Pintsuk, I. Bobin-Vastra, S. Constans, P. Gavila, M. Rödig, and B. Riccardi, “Qualification and post-mortem characterization of tungsten mock-ups exposed to cyclic high heat flux loading,” Fusion Eng. Des., vol. 88, no. 9–10, pp. 1858–1861, Oct. 2013.

[8] M. Li and J.-H. You, “Interpretation of the deep cracking phenomenon of tungsten monoblock targets observed in high-heat-flux fatigue tests at 20 MW/m2,” Fusion Eng. Des., vol. 101, pp. 1–8, Dec. 2015.

[9] M. Li and J.-H. You, “Structural impact of armor monoblock dimensions on the failure behavior of ITER-type divertor target components: Size matters,” Fusion Eng. Des., vol. 113, pp. 162–170, Dec. 2016.

[10] ITER Structural Design Criteria for In-vessel Components (SDC-IC) Appendix A: Materials Design Limit Data,G 74 MA 8 01-05-28 W 0.2, 2013.

[11] J. Du, Y. Yuan, M. Wirtz, J. Linke, W. Liu, and H. Greuner, “FEM study of recrystallized tungsten under ELM-like heat loads,” J. Nucl. Mater., vol. 463, pp. 219–222, Aug. 2015.

[12] J. Reiser et al., “Tungsten foil laminate for structural divertor applications – Tensile test properties of tungsten foil,” J. Nucl. Mater., vol. 434, no. 1–3, pp. 357–366, Mar. 2013.

[13] J. Farre, M. Lamaison, A. Cosculluela, and J.-L. Lataillade, “Étude de la transition fragile-ductile d’un tungstène,” J. Phys. IV Colloq., vol. 07, no. C3, pp. C3-879-C3-884, 1997.

[14] M. Wirtz et al., “Material properties and their influence on the behaviour of tungsten as plasma facing material,” Nucl. Fusion, vol. 57, no. 6, p. 066018, 2017.

[15] Endommagement et rupture des matériaux. Volume 1, Généralités, matériaux métalliques - Michel Clavel, Philippe Bompard. .

[16] Forschungszentrum Karlsruhe, Nuclear Fusion Programme Annual Report of the Association Forschungszentrum Karlsruhe/EURATOM January 2006 – December 2006,Wissenschaftliche Berichte FZKA 7291 EUR 22705 EN. .

[17] J. R. S. Thom, W. M. Walker, T. A. Fallon, and G. F. S. Reising, “Boiling in subcooled water during flow up heated tubes or annuli,” Proc Inst Mech Eng, vol. 180, no. PART 3C, pp. 226–246, 1965.

[18] K. V. U. Praveen and V. Singh, “Effect of heat treatment on Coffin–Manson relationship in LCF of superalloy IN718,” Mater. Sci. Eng. A, vol. 485, no. 1, pp. 352–358, Jun. 2008.

[19] ITER Material Properties Handbook, ITER Document No. S 74 MA 2.